

# The Relationship between Transannular Secondary Bonding Strength and Conformation in Diphenyldithiophosphinate Stibocanes $\mathbf{X}(\text{CH}_2\text{CH}_2\text{S})_2\text{SbS}_2\text{PPh}_2$ ( $\mathbf{X} = \text{O, S}$ )

Miguel-Angel Muñoz-Hernández,\* Raymundo Cea-Olivares, and Simón Hernández-Ortega

México, D. F./México, Instituto de Química, Universidad Nacional Autónoma de México

Received January 22nd, 1996.

**Abstract.** The two stibocanes 1-oxa-4,6-dithia-5-stibocane diphenyldithiophosphinate  $\text{O}(\text{CH}_2\text{CH}_2\text{S})_2\text{SbS}_2\text{PPh}_2$  **1** and 1,3,6-trithia-2-stibocane diphenyldithiophosphinate  $\text{S}(\text{CH}_2\text{CH}_2\text{S})_2\text{SbS}_2\text{PPh}_2$  **2** were prepared from the corresponding chloro oxa- and thia-stibocanes **3** and **6**, and the ammonium salt of diphenyldithiophosphinic acid in  $\text{CH}_2\text{Cl}_2$ . **1** and **2** were characterized by IR, EI-MS and multinuclear NMR ( $^1\text{H}$ ,  $^{13}\text{C}$ ,  $^{31}\text{P}({}^1\text{H})$ ). The crystalline state of **1** features two  $\text{Sb}_1 \cdots \text{S}_1$  intermolecular interactions [3.987(2) Å] that results in a dimer. Alongside **1** displays both an endocyclic, transannular  $\text{Sb}_1 \cdots \text{O}_1$  interaction [2.555(6) Å] and an exocyclic  $\text{Sb}_1 \cdots \text{S}_4$  secondary interaction [3.327(2) Å]. The coordination geometry at the antimony could be described as  $\text{AX}_4\text{YE}$   $\psi$ -trigonal bipyramidal geometry with  $\text{A} = \text{Sb}$ ,  $\text{X} = \text{S}_1$ ,  $\text{S}_2$ ,  $\text{S}_3, \text{O}_1$ ;  $\text{Y} = \text{S}_4$ ;  $\text{S}_1, \text{S}_2$  and the lone pair lays on the equatorial

plane with  $\text{O}_1$  and  $\text{S}_4$  in axial positions. The  $\text{Sb}_1 \cdots \text{S}_4$  secondary bonding is face capping one of the planes form by the lone pair,  $\text{S}_2$  and  $\text{S}_3$  of the trigonal bipyramidal. **2** also displays both an endocyclic, transannular  $\text{Sb}_1 \cdots \text{S}_2$  interaction [2.949(3) Å] and an exocyclic  $\text{Sb}_1 \cdots \text{S}_5$  secondary interaction [3.216(3) Å]. The antimony becomes five-coordinate, giving the  $\text{AX}_4\text{YE}$   $\psi$ -trigonal bipyramidal geometry with  $\text{S}_1, \text{S}_3$  and the lone pair laying on the equatorial plane with  $\text{S}_2$  and  $\text{S}_4$  in axial positions. The  $\text{Sb}_1 \cdots \text{S}_5$  also here is face capping the plane form by the lone pair,  $\text{S}_3$  and  $\text{S}_4$  of the trigonal bipyramidal.

The conformation of the eight membered ring in **2** is boat-chair. In **1** the main conformation is chair-planar.

**Keywords:** Stibocanes; conformational analysis; x-ray structures

## Die Beziehung zwischen starker transannularer sekundärer Bindung und Konformation in Diphenyldithiophosphinatstibocanen $\mathbf{X}(\text{CH}_2\text{CH}_2\text{S})_2\text{SbS}_2\text{PPh}_2$ ( $\mathbf{X} = \text{O, S}$ )

**Inhaltsübersicht.** Die beiden Stibocane 1-Oxa-4,6-dithia-5-stibocan-diphenyldithiophosphinat  $\text{O}(\text{CH}_2\text{CH}_2\text{S})_2\text{SbS}_2\text{PPh}_2$  **1** und 1,3,6-Trithia-2-stibocan-diphenyldithiophosphinat  $\text{S}(\text{CH}_2\text{CH}_2\text{S})_2\text{SbS}_2\text{PPh}_2$  **2** wurden aus den entsprechenden Chloro-oxa- und -thia-stibocanen **3** und **6** sowie dem Ammoniumsalz der Diphenyldithiophosphinsäure in  $\text{CH}_2\text{Cl}_2$  dargestellt. **1** und **2** wurden durch IR, EI-MS und Multikern-NMR-( $^1\text{H}$ ,  $^{13}\text{C}$ ,  $^{31}\text{P}({}^1\text{H})$ ) Spektren charakterisiert. Die Kristallstruktur von **1** zeigt zwei  $\text{Sb}_1 \cdots \text{S}_1$  intermolekulare Wechselwirkungen [3.987(2) Å] so daß sich ein dimeres Molekül ergibt sowie eine endocyclische, transannulare  $\text{Sb}_1 \cdots \text{O}_1$  [2.555(6) Å] und eine exocyclische  $\text{Sb}_1 \cdots \text{S}_4$  sekundäre Wechselwirkung [3.327(2) Å]. Die Koordination am Antimon kann als  $\text{AX}_4\text{YE}$   $\psi$ -trigonal bipyramidal Geometrie beschrieben werden, mit  $\text{A} = \text{Sb}$ ,  $\text{X} = \text{S}_1, \text{S}_2, \text{S}_3, \text{O}_1$ ;  $\text{Y} = \text{S}_4$ .  $\text{S}_1, \text{S}_2$  und das freie Elektronenpaar liegen in der äquatorialen

Ebene,  $\text{O}_1$  und  $\text{S}_3$  besetzen die axialen Positionen. Die sekundäre Bindung  $\text{Sb}_1 \cdots \text{S}_4$  liegt über einer Ebene, die von dem freien Elektronenpaar der trigonalen Bipyramide,  $\text{S}_2$  und  $\text{S}_3$  gebildet wird. Molekül **2** zeigt ebenfalls eine endocyclische, transannulare  $\text{Sb}_1 \cdots \text{S}_2$  [2.949(3) Å] und eine exocyclische  $\text{Sb}_1 \cdots \text{S}_5$  sekundäre Wechselwirkung [3.216(3) Å]. Antimon ist hier ebenfalls fünffach koordiniert, wodurch sich eine  $\text{AX}_4\text{YE}$   $\psi$ -trigionale bipyramidal Geometrie ergibt, mit  $\text{S}_1, \text{S}_3$  und dem freien Elektronenpaar in der äquatorialen Ebene und mit  $\text{S}_2$  und  $\text{S}_4$  in den axialen Positionen. Die sekundäre Bindung  $\text{Sb}_1 \cdots \text{S}_5$  liegt auch hier über einer Ebene, die von dem freien Elektronenpaar der trigonalen Bipyramide,  $\text{S}_3$  und  $\text{S}_4$  gebildet wird.

Die Konformation des Achtringes in **2** ist Wanne-Sessel. In **1** ist die Konformation des Achtringes Sessel-planar.

## Introduction

A variety of metallocanes of the type shown in Figure 1, where the transannular atom is  $X = O, S, NR$  and  $M = Ge, Sn, Pb, P, As, Sb, Bi$ , have been prepared and characterized [1–6]. In all these compounds there is a strong 1, 5 transannular interaction, which has been studied mainly by vibrational spectroscopy and single-crystal X-ray diffraction.

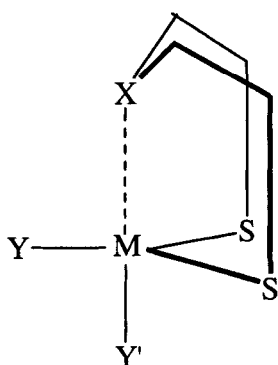


**Fig. 1** Metallocanes of the type  $X(CH_2CH_2S)_2MYY'$ ,  $X = O, S$ ;  $M = Ge, Sn, Pb, P, As, Sb$  and  $Bi$ ;  $Y, Y' = \text{halogen, alkyl and aryl}$

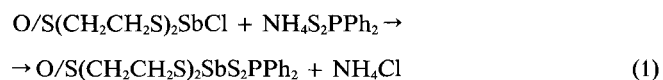
The 1, 5 transannular interaction in these metallocanes is a stabilizing factor in comparison with the situation found in the cyclooctane ring, that presents in the 1, 5 positions additional Pitzer tension [7]. The conformation adopted by the 8 membered ring has been investigated in solution by  $^1\text{H-NMR}$  and in solid state by single crystal X-ray spectroscopy [8]. Such studies have revealed that the 8-membered metallo ring  $XC_4S_2M$  ( $X = O, S$ ) exhibit various conformations with extreme situations in the boat-boat, boat-chair and chair-chair conformations [8, 9]. For the oxa and thia-stibocanes it is possible to propose a relationship between the strength of the transannular interaction<sup>1</sup>) and the conformation adopted by the eight membered ring, because the oxa-stibocanes which possess a longer transannular interaction tends to present the chair-chair conformation while the thia-stibocanes with a shorter one, the boat-chair (e.g.  $O(CH_2CH_2S)_2 \cdot SbCl$  **3**, 26% longer than  $\Sigma cov$  vs.  $S(CH_2CH_2S)_2SbCl$  **6** 17%) [10, 11]. This relationship is supported by the dithiolate bridge-type compound  $O(CH_2CH_2S)_2Sb-SCH_2 \cdot CH_2OCH_2CH_2S-Sb(SCH_2CH_2)O$  **5** [8], where in the heterocycle with the longer  $Sb \cdots O$  transannular secondary bonding [2.734(3) vs. 2.637(4) Å] the conformation is chair-chair while in the shorter one is boat-chair.

In order to gain more insight in the relation between the strength of the transannular interaction and the con-

formation, it would be interesting to replace the halide atom in the stibocanes **3** and **6** with potentially sulfur bidentate ligands such as dithiocarbamates, dithiophosphates and dithiophosphinates. These ligands may induce a competition for the residual affinity of the antimony in the 8 membered ring that could affect the coordination number around the metal, the strength of the endocyclic transannular interaction, and the conformation adopted by the 8 membered heterocycle. We previously reported the synthesis and characterization of some dithiophosphate metallocane derivatives [12]. Here we describe the synthesis and spectroscopic characterization of 1-oxa-4,6-dithia-5-stibocene diphenyldithiophosphinate  $O(CH_2CH_2S)_2SbS_2PPh_2$  **1** and 1,3,6-trithia-2-stibocene diphenyldithiophosphinate  $S(CH_2CH_2S)_2SbS_2PPh_2$  **2**, as well as their crystal and molecular structures.

## Results and Discussion

The oxa and thia-stibocene diphenyldithiophosphinates were prepared from the chloro oxa- and thia-stibocanes **3** and **6** [10, 11], and the ammonium salt of diphenyldithiophosphinic acid [13] in  $CH_2Cl_2$  according to equation (1) ( $X = O$  or  $S$ ).



The diphenyldithiostibocanes are air stable, colorless, crystalline solids, soluble in organic solvents (e.g.  $CH_2CH_2$ ,  $CH_3Cl$ , benzene, but not in hexane). The compounds were characterized by IR, EI-MS and multinuclear NMR ( $^1\text{H}$ ,  $^{13}\text{C}$ ,  $^{31}\text{P}[^1\text{H}]$ ). The crystal and molecular structures of 1-oxa-4,6-dithia-5-stibocene diphenyldithiophosphinate,  $O(CH_2CH_2S)_2SbS_2PPh_2$ , **1** and 1,3,6-trithia-2-stibocene diphenyldithiophosphinate,  $S(CH_2CH_2S)_2SbS_2PPh_2$ , **2** were determined.

Relevant infrared bands of the new compounds were assigned by comparison with the spectra of the starting materials and literature data [14]. Two medium to strong absorption bands were assigned to symmetrical and asymmetrical phosphorus-sulfur stretching vibrations [14]. The difference between these vibrations,  $\Delta$ , has been used for estimating the  $\pi$ -electron-density delocalisation in the fragment  $PS_2$  [14]. For the oxa and thia-stibocene derivatives  $\Delta = 125$  and  $126 \text{ cm}^{-1}$  respectively. The  $\Delta$  value in these stibocanes is compatible with a small  $\pi$ -electron-density delocalisation of the  $PS_2$  moiety of the ligand. Characteristic absorption bands for the CXC group in the stibocanes **1** and **2** are also present [15, 16].

The electron impact mass spectrum (EI-MS) for the stibocanes **1** and **2** shows ion fragments from the 8 membered ring  $X(CH_2CH_2S)_2Sb$ , i.e.  $X(CH_2CH_2S)_2Sb^+$  and  $\overline{XCH_2CH_2SSb}^+$  which have been found in other stibocanes [15, 16], and from the diphenyldithiophosphinate ligand. No fragments were found at higher mass than the molecular mass which is consistent with an essentially monomeric nature of the compounds investigated.

For the 8 membered ring of the stibocanes **1** and **2**, the  $^1\text{H-NMR}$  spectra exhibit the anticipated resonances in the ap-

<sup>1</sup>) In order to compare the strength of the transannular interaction it is used the sum of the covalent radii  $\Sigma cov$ .  $Sb-O \Sigma cov = 2.00 \text{ \AA}$ ,  $Sb-S \Sigma cov = 2.45 \text{ \AA}$  (ref. [8])

properite relative intensities expected for the ABCD spin system of the  $-\text{SCH}_2\text{CH}_2\text{X}-$  fragment [17]. The aryl groups attached to phosphorus are equivalent on the  $^1\text{H}$  and  $^{13}\text{C}$  NMR time scale and show the expected multiplicity due to the phosphorus-proton, and phosphorus-carbon couplings. Only one sharp resonance was observed in the  $^{31}\text{P}$  NMR spectra.

### X-ray Structures of the Stibocanes **1** and **2**

The stibocanes **1** and **2** were amenable to study by single-crystal X-ray diffraction, and a summary of crystallographic and structure solution data is presented in Table 1. Fractional coordinates and thermal parameters have been assembled in Tables 2 and 3. Selected bond distances and angles for **1** and **2** are given in Tables 4 and 5, respectively.

The oxa-stibocane **1** crystallizes in the monoclinic space group  $\text{P}2_1/n$  with 4 molecules in the unit cell. One molecule is illustrated in Figure 2 along with the atom numbering scheme. The crystalline state of **1** features two  $\text{Sb}1 \cdots \text{S}1\text{a}$  intermolecular interactions [ $3.987(2) \text{ \AA}$ ] that results in a dimer, which is illustrated in Figure 3. The molecules in the dimer are related by the  $2_1$  screw axis. Alongside **1** displays both an endocyclic, transan-

nular  $\text{Sb}1 \cdots \text{O}1$  interaction [ $2.555(6) \text{ \AA}$ ] and an exocyclic  $\text{Sb}1 \cdots \text{S}4$  secondary interaction [ $3.327(2) \text{ \AA}$ ]. The transannular interaction in **1** is slightly longer than in the chloro oxa-stibocane **3** [ $2.529 \text{ \AA}$ ] [10, 11], but shorter than in the phenyl derivative  $\text{O}(\text{CH}_2\text{CH}_2\text{S})_2\text{SbPh}$  **4** [ $2.942(4) \text{ \AA}$ ] [1] and the dithiolate bridge-type compound **5** [8]. The competition between  $\text{S}4$  and  $\text{O}1$  for coordination to antimony in the stibocane **1** accounts for the slightly longer transannular secondary bonding in comparison to **3**. The phosphorus-sulfur bonds in **1** are non-equivalent  $\text{P}=\text{S}3$  [ $2.073(3) \text{ \AA}$ ] and  $\text{P}=\text{S}(4)$  [ $1.956(2) \text{ \AA}$ ], this latter value is intermediate between a double  $\text{P}=\text{S}$  and a single  $\text{P}=\text{S}$  bond [18].

If the secondary interactions are neglected, the antimony atom displays the trigonal pyramidal geometry found in  $\text{SbX}_3$  molecules [19, 20], but with nonequivalent  $\text{S}=\text{Sb}=\text{S}$  bond angles [ $86.1(1)$ ,  $88.4(1)$ , and  $102.7(1)^\circ$ ]. If secondary bonding is not neglected, the antimony becomes five-coordinate, giving the  $\text{AX}_4\text{YE}$   $\psi$ -trigonal bipyramidal geometry with  $\text{A} = \text{Sb}$ ,  $\text{X} = \text{S}1$ ,  $\text{S}2$ ,  $\text{S}3$ ,  $\text{O}1$ ;  $\text{Y} = \text{S}4$ ;  $\text{S}1$ ,  $\text{S}2$  and the lone pair lays on the equatorial plane with  $\text{O}1$  and  $\text{S}4$  in axial positions. The  $\text{Sb}1 \cdots \text{S}4$  secondary bonding is face capping one of the

**Table 1** Crystallographic and structure solution data for the stibocanes **1** and **2**

	<b>1</b>	<b>2</b>
Compound formula	$\text{C}_{16}\text{H}_{18}\text{OPS}_4\text{Sb}$	$\text{C}_{16}\text{H}_{18}\text{PS}_5\text{Sb}$
M	507.3	523.3
Crystal System	Monoclinic	Orthorhombic
Space group	$\text{P}2_1/n$	$\text{P}2_12_12_1$
a/ $\text{\AA}$	9.306(2)	8.812(2)
b/ $\text{\AA}$	12.592(2)	13.269(2)
c/ $\text{\AA}$	17.753(3)	17.529(2)
U/ $\text{\AA}^3$	2017.8(4)	2049.6(4)
$\theta$ range for cell/ $^\circ$	2.52 – 12.53	5.28 – 12.52
Z	4	4
$D_c/\text{gcm}^{-3}$	1.663	1.696
F(000)	1000	1040
$\mu(\text{Mo-K}\alpha)/\text{mm}^{-1}$	1.860	1.929
Scan mode	$\omega$	$\omega$
$\theta$ range/ $^\circ$	1.5 – 25	1.5 – 25
Crystal size/mm	$0.36 \times 0.28 \times 0.08$	$0.32 \times 0.12 \times 0.11$
Range of transmission coefficients	0.6795 – 0.8334	0.6460 – 0.6969
Reflections collected	3782	2094
Unique reflections	3548	2073
Refined reflections	2250	1599
hkl ranges	0 to 11, 0 to 14, –21 to 20	0 to 10, 0 to 15, 0 to 20
$R_{\text{merge}}$	0.0244	0.000
No. of refined parameters	208	209
Final R ('observed' data) <sup>a</sup>	0.0331	0.0416
Final R' (all data) <sup>b</sup>	0.0518	0.0646
Goodness of fit, S <sup>c</sup>	1.01	1.08
Maximum/minimum largest remaining feature in electron density map/e $\text{\AA}^{-3}$	0.42, –0.48	0.46, –0.45

<sup>a</sup>) Conventional  $R = \sum ||F_o|| - |F_c|| / \sum |F_o|$  for reflections having  $F_o^2 > 2\sigma(F_o^2)$  ('observed' reflections).

<sup>b</sup>)  $R' = [\sum w(F_o^2 - F_c^2)^2 / \sum w(F_o^2)]^{1/2}$ .

<sup>c</sup>) On  $F^2$  values for all data.

**Table 2** Atomic coordinates ( $\times 10^4$ ) and equivalent isotropic displacement coefficients ( $\text{\AA}^2 \times 10^3$ ) for  $\text{O}(\text{CH}_2\text{CH}_2\text{S})\text{SbS}_2\text{PPh}_2$ 

Atom	x	y	z	U(eq)
Sb	6562(1)	3459(1)	5673(1)	48(1)
S(1)	6579(2)	5322(1)	6049(1)	67(1)
S(2)	8449(3)	2690(2)	6718(2)	87(1)
S(3)	8565(3)	3954(2)	5017(1)	84(1)
S(4)	6529(2)	1833(1)	4192(1)	55(1)
O(1)	5348(6)	3450(5)	6818(3)	74(2)
P(1)	8257(2)	2728(1)	2414(1)	44(1)
C(1)	5157(17)	5251(9)	6542(10)	154(9)
C(2)	4925(15)	4482(10)	6991(8)	134(7)
C(3)	6203(11)	2908(9)	7461(5)	93(4)
C(4)	7462(19)	2630(23)	7420(11)	361(20)
C(11)	9980(7)	1990(6)	4000(4)	52(2)
C(12)	9951(9)	922(6)	4239(4)	663(3)
C(13)	11259(10)	347(8)	4305(5)	83(4)
C(14)	12587(11)	862(9)	4552(6)	96(4)
C(15)	12623(10)	1910(10)	4701(6)	100(5)
C(16)	11345(9)	2488(7)	4643(5)	76(3)
C(21)	8194(6)	3357(5)	3290(3)	45(2)
C(22)	7372(8)	2901(6)	2618(4)	60(2)
C(23)	7409(10)	3317(8)	1897(4)	80(3)
C(24)	8229(10)	4205(7)	1856(5)	76(3)
C(25)	9024(10)	4679(6)	2522(5)	73(3)
C(26)	9018(8)	4273(5)	3237(4)	60(3)

**Table 3** Atomic coordinates ( $\times 10^4$ ) and equivalent isotropic displacement coefficients ( $\text{\AA}^2 \times 10^3$ ) for  $\text{S}(\text{CH}_2\text{CH}_2\text{S})\text{SbS}_2\text{PPh}_2$ 

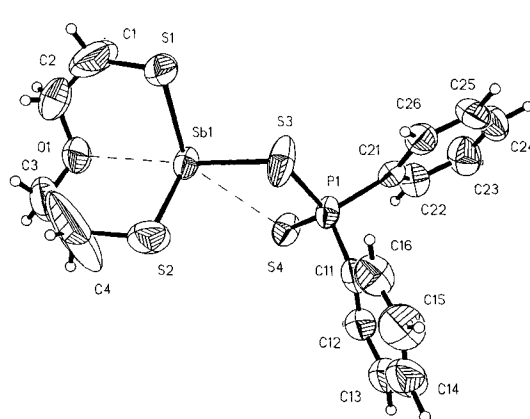
Atom	x	y	z	U(eq)
Sb(1)	7528(1)	1670(1)	9248(1)	36(1)
S(1)	6409(4)	2780(3)	10221(2)	49(1)
S(2)	7464(6)	329(2)	10588(2)	55(1)
S(3)	5277(4)	655(3)	8978(2)	55(1)
S(4)	6843(4)	3183(2)	8362(2)	43(1)
S(5)	7984(4)	1054(2)	7489(2)	49(1)
P(1)	6928(4)	2355(2)	7369(2)	36(1)
C(1)	7228(23)	2301(10)	11078(7)	69(6)
C(2)	6920(22)	1239(11)	11307(8)	77(7)
C(3)	5703(17)	-257(10)	10374(9)	64(5)
C(4)	4605(16)	383(11)	9924(8)	66(5)
C(11)	7802(11)	3135(7)	6637(6)	35(4)
C(12)	7807(16)	2775(9)	5902(6)	52(5)
C(13)	8526(18)	3321(14)	5327(8)	69(6)
C(14)	9187(19)	4246(14)	5476(10)	74(7)
C(15)	9141(16)	4585(12)	6195(10)	70(6)
C(16)	8472(16)	4050(10)	6795(8)	57(5)
C(21)	4976(14)	2205(8)	7053(7)	40(4)
C(22)	4272(16)	1273(10)	6998(7)	49(4)
C(23)	2773(19)	1248(12)	6781(8)	69(6)
C(24)	1917(20)	2099(13)	6645(9)	73(6)
C(25)	2645(20)	3030(12)	6699(7)	65(5)
C(26)	4135(15)	3102(9)	6889(7)	48(4)

**Table 4** Selected interatomic distances ( $\text{\AA}$ ) and angles ( $^\circ$ ) in  $\text{O}(\text{CH}_2\text{CH}_2\text{S})\text{SbS}_2\text{PPh}_2$ 

Sb(1)—S(1)	2.438(2)	S(1)—Sb(1)—S(2)	102.7(1)
Sb(1)—S(2)	2.425(2)	Sb(1)—S(1)—C(1)	97.6(4)
Sb(1)—S(3)	2.505(3)	S(1)—C(1)—C(2)	113.9(3)
P(1)—S(3)	2.073(3)	C(1)—C(2)—O(1)	117.0(1)
P(1)—S(4)	1.956(2)	C(2)—O(1)—C(3)	113.8(8)
Sb(1) ··· O(1)	2.555(6)	C(3)—C(4)—O(1)	117.0(1)
Sb(1) ··· S(4)	3.327(2)	C(3)—C(4)—S(2)	135.1(1)
Sb(1) ··· S(1 a)	3.987(2)	C(4)—S(2)—Sb(1)	99.0(6)
		S(2)—Sb(1)—S(3)	88.4(1)
		S(1)—Sb(1)—S(3)	86.1(1)
		P(1)—S(3)—Sb(1)	98.1(1)
		S(3)—Sb(1) ··· O(1)	153.4(1)
		S(1)—Sb(1) ··· O(1)	76.2(2)
		S(2)—Sb(1) ··· O(1)	76.6(1)
		S(4) ··· Sb(1)—S(1)	143.8(1)
		S(4) ··· Sb(1)—S(2)	103.1(1)
		S(4) ··· Sb(1)—S(3)	69.5(1)
		S(4) ··· Sb1 ··· O(1)	134.9(1)

**Table 5** Selected interatomic distances ( $\text{\AA}$ ) and angles ( $^\circ$ ) in  $\text{S}(\text{CH}_2\text{CH}_2\text{S})\text{SbS}_2\text{PPh}_2$ 

Sb(1)—S(1)	2.460(3)	S(1)—Sb(1)—S(3)	98.0(1)
Sb(1)—S(3)	2.444(4)	Sb(1)—S(1)—C(1)	102.1(5)
Sb(1)—S(4)	2.608(3)	S(1)—C(1)—C(2)	120.0(1)
P(1)—S(4)	2.061(4)	C(1)—C(2)—S(2)	114.0(1)
P(1)—S(5)	1.973(4)	C(2)—S(2)—C(3)	102.0(8)
Sb(1) ··· S(2)	2.949(3)	C(3)—C(4)—S(2)	116.0(1)
Sb(1) ··· S(5)	3.216(3)	C(3)—C(4)—S(3)	114.0(1)
Sb(1) ··· S(1 a)	3.618(4)	C(4)—S(3)—Sb(1)	101.5(5)
		S(3)—Sb(1)—S(4)	97.0(1)
		S(1)—Sb(1)—S(4)	81.9(1)
		P(1)—S(4)—Sb(1)	94.8(1)
		S(3)—Sb(1) ··· S(4)	96.9(1)
		S(1)—Sb(1) ··· S(2)	78.5(1)
		S(3)—Sb(1) ··· S(2)	78.8(1)
		S(5) ··· Sb(1)—S(1)	150.2(1)
		S(5) ··· Sb(1)—S(2)	127.8(1)
		S(5) ··· Sb(1)—S(4)	69.8(1)
		S(4) ··· Sb1 ··· S(2)	134.9(1)

**Fig. 2** ORTEP view of  $\text{O}(\text{CH}_2\text{CH}_2\text{S})\text{SbS}_2\text{PPh}_2$

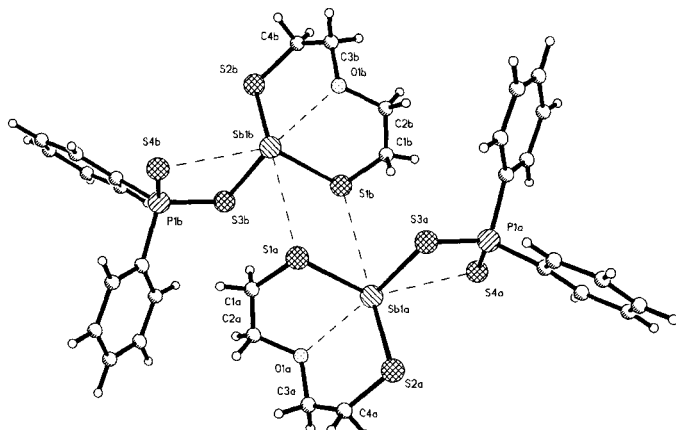


Fig. 3 Dimeric structure of  $O(CH_2CH_2S)_2SbS_2PPh_2$

planes form by the lone pair, S2 and S3 of the trigonal bipyramidal.

The thia-stibocane **2** crystallizes in the orthorhombic space group  $P2_12_12_1$ , with 4 molecules in the unit cell. The molecules in the crystal are aligned along the three  $2_1$  screw axes. Perpendicular to these axes, the molecules forms infinite chains through  $Sb1 \cdots S1a$  intermolecular interactions [3.618(2) Å] (Fig. 4). One molecule is illustrated in Figure 5 along with the atom numbering scheme. The molecule **2** also displays both an endocyclic, transannular  $Sb1 \cdots S2$  interaction [2.949(3) Å] and an exocyclic  $Sb1 \cdots S5$  secondary interaction [3.216(3) Å], the transannular interaction in **2** is longer than in the chloro and bromo thia-stibocanes  $S(CH_2CH_2S)_2SbCl/Br$  **6**, **6a** (2.83–2.88 Å),[10, 3] but shorter than in the phenyl and p-nitrophenyl derivatives  $S(CH_2CH_2S)_2SbPh/pnPh$  **7**, **7a** (3.19–3.36 Å) [2, 3]. The competition between S4 and S2 for coordination to antimony in the stibocane **2** accounts again for the slightly longer transannular secondary bonding found in relation to **6** and **6a**. The phosphorus-sulfur bonds in **2** are non-equivalent  $P1-S4$  [2.061(4) Å] and  $P1-S5$  [1.973(4) Å] this latter value is as in **1** intermediate between a double P=S and a single P—S bond [18].

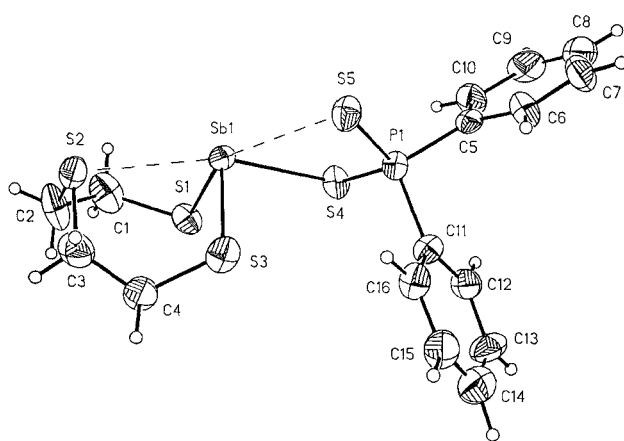


Fig. 4 ORTEP view of  $S(CH_2CH_2S)_2SbS_2PPh_2$

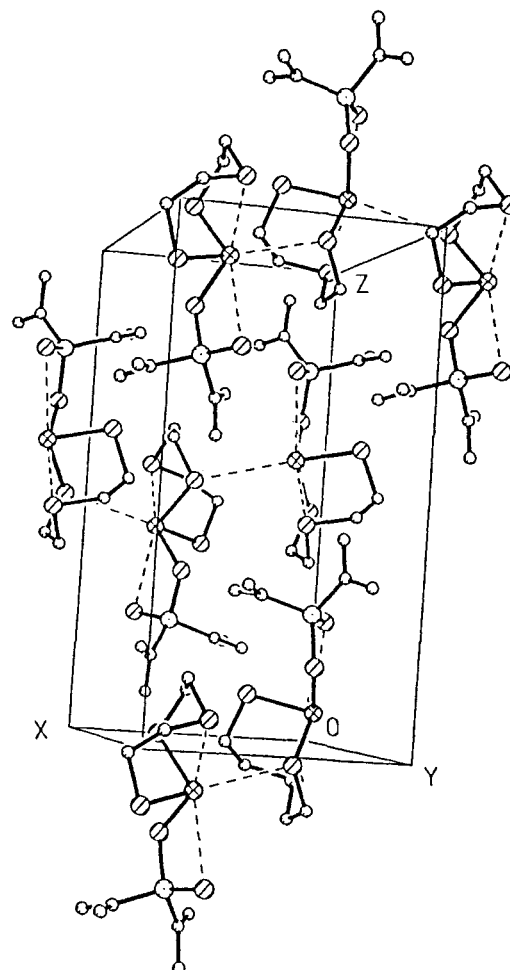


Fig. 5 Crystal structure of  $S(CH_2CH_2S)_2SbS_2PPh_2$

Ignoring the secondary interactions, the antimony displays a trigonal pyramidal geometry with nonequivalent S—Sb—S bond angles [81.9(1), 97.0(1), and 98.0(1)°]. If secondary bonding is not neglected, the antimony becomes five-coordinate, giving the  $AX_4YE$   $\psi$ -trigonal bipyramidal geometry with S1, S3 and the lone pair laying on the equatorial plane with S2 and S4 in axial positions. The  $Sb1 \cdots S5$  also here is face capping the plane form by the lone pair, S3 and S4 of the trigonal bipyramidal.

The conformation of the 8 membered ring in **2** is boat-chair, as has been found in other related thia-stibocanes [8]. The decrease in strength of the transannular bonding when is replaced S for O in the stibocane **1** could be the source of the greater isotropic and anisotropic vibration parameters of the carbon atoms that comprise the 8 membered ring. An interesting feature is that the anisotropic motion is more severe (C4) just in the part of the ring where there is not transannular interactions (see Figure 4). The main conformation in the fragment of the ring that comprises the Sb1, S2, C3, C4 and O1 is planar<sup>2)</sup> and is the first example of a stibocane of the

<sup>2)</sup> The main deviation from the plane is 0.0442 Å.

type shown in Figure 1 which presents such conformation. Therefore the conformation of the eight membered ring could be described as a chair-planar as has been described previously for the oxa-stanocane O(CH<sub>2</sub>CH<sub>2</sub>S)<sub>2</sub>SnPh<sub>2</sub> [21].

## Experimental Section

### General Considerations

Starting compounds O/S(CH<sub>2</sub>CH<sub>2</sub>SH)<sub>2</sub> and SbCl<sub>3</sub> were purchased and used as received. Solvents were dried before used. The chloro stibocanes were obtained using published procedures [10, 11]. Ammonium diphenyldithiophosphinate was obtained by bubbling gaseous ammonia into the benzene solution of the free acid [13]. Elemental analyses (C, H) were performed by Galbraith Laboratories, Inc. (Knoxville, TN). IR spectra (4000–200 cm<sup>-1</sup>) were recorded on KBr pellets using a Perkin-Elmer 282B spectrometer. 70 eV Electron-impact mass spectra were recorded using a Hewlett-Packard MS-598 instrument. <sup>1</sup>H, <sup>13</sup>C and <sup>31</sup>P NMR spectra were obtained in CDCl<sub>3</sub> solution using a Varian Gemini 300 spectrometer operating at 299.949, 75.3 and 121.4 MHz, respectively. Tetramethylsilane and H<sub>3</sub>PO<sub>4</sub> (85%) were used as external standards.

### Synthesis of 1-oxa-4, 6-dithia-5-stibocane Diphenyldithiophosphinate 1

Stoichiometric amounts of O(CH<sub>2</sub>CH<sub>2</sub>S)<sub>2</sub>SbCl (0.30 g, 1 mmol) and ammonium diphenyldithiophosphinate (0.27 g, 1 mmol) in CH<sub>2</sub>Cl<sub>2</sub> (20 cm<sup>3</sup>) were stirred for 12 h. The reaction mixture was filtered off to remove the resulting NH<sub>4</sub>Cl and the clear filtrate was evaporated at low pressure. The resulting powder was recrystallised from a CH<sub>2</sub>Cl<sub>2</sub>/n-hexane mixture afforded colorless crystals of O(CH<sub>2</sub>CH<sub>2</sub>S)<sub>2</sub>Sb<sub>2</sub>PPH<sub>2</sub> **1** (0.36 g, 69%), mp 143–145 °C. Anal. calcd for C<sub>16</sub>H<sub>18</sub>OPS<sub>4</sub>Sb: C, 37.88; H, 3.58 %. Found: C, 37.59; H, 3.79%.

IR (KBr):  $\nu_{as}(PS_2)$  605 w,  $\nu_s(PS_2)$  480 m,  $\nu_{as}(COC)$  1090 s, 1070 s,  $\nu_s(COC)$  1010 m, 990 m, 975 m,  $\nu(MS)$  340 w, 310 m, 285 m cm<sup>-1</sup>. <sup>1</sup>H-NMR (CDCl<sub>3</sub>):  $\delta$  3.08 ppm (4H, m, OCH<sub>2</sub>), 3.63 ppm (2H, ddd, SCH), 4.17 ppm (2H, ddd, SCH), 7.63 ppm [6H, m, P—C<sub>6</sub>H<sub>5</sub> (meta + para)], 7.91 ppm [4H, ddd, P—C<sub>6</sub>H<sub>5</sub> (ortho)], <sup>3</sup>J(HH) = 7.9, <sup>4</sup>J(HH) = 1.8, <sup>3</sup>J(PH) = 14.8. <sup>13</sup>C-NMR (CDCl<sub>3</sub>):  $\delta$  29.96 ppm (2C, s, CH<sub>2</sub>S), 74.26 ppm (2C, s, CH<sub>2</sub>O), 128.28 ppm [2C, d, C<sub>m</sub>, <sup>3</sup>J(PC) = 13.7], 130.90 ppm [2C, d, C<sub>o</sub>, <sup>2</sup>J(PC) = 11.6], 131.36 ppm [1C, s, C<sub>p</sub>], 137.26 ppm [1C, d, C<sub>i</sub>, <sup>1</sup>J(PC) = 84.9]. <sup>31</sup>P NMR (CDCl<sub>3</sub>):  $\delta$  58.1 ppm. EI-MS (70 eV): m/z = 506 ( $M^+$ , 6%), 370 (Ph<sub>2</sub>PS<sub>2</sub>Sb<sup>+</sup>, 78%), 257 [O(CH<sub>2</sub>CH<sub>2</sub>S)<sub>2</sub>Sb<sup>+</sup>, 5%], 249 (Ph<sub>2</sub>PS<sub>2</sub><sup>+</sup>, 4%), 217 (Ph<sub>2</sub>PS<sup>+</sup>, 100%), 197 (OCH<sub>2</sub>CH<sub>2</sub>SSb<sup>+</sup>, 34%), 185 (Ph<sub>2</sub>P<sup>+</sup>, 26%), 153 (SbS<sup>+</sup>, 32%).

### Synthesis of 1,3,6-trithia-2-stibocane Diphenyldithiophosphinate 2

The synthesis and separation was carried out similarly to the oxa-stibocane **1**, afforded colorless crystals of S(CH<sub>2</sub>CH<sub>2</sub>S)<sub>2</sub>·Sb<sub>2</sub>PPH<sub>2</sub> **2** (0.33 g, 63%) mp 180–182 °C. Anal. calcd for C<sub>16</sub>H<sub>18</sub>PS<sub>5</sub>Sb: C, 36.72; H, 3.47%. Found: C, 36.71; H, 3.58%. IR (KBr):  $\nu_{as}(PS_2)$  612 w,  $\nu_s(PS_2)$  484 w,  $\nu_{as}(CSC)$  1098 m, 1067 w, 1023 w, 924 w, 895 w, 838 w, 829 w,  $\nu_s(CSC)$  747 m, 709 s,  $\nu(MS)$  343 m, 314 w, 286 m cm<sup>-1</sup>. <sup>1</sup>H-NMR (CDCl<sub>3</sub>):  $\delta$

2.81 ppm (2H, d), 3.24 (4H, m), 3.50 ppm (2H, ddd), 7.43 ppm [6H, m, P—C<sub>6</sub>H<sub>5</sub> (meta + para)], 7.94 ppm [4H, ddd, P—C<sub>6</sub>H<sub>5</sub> (ortho)], <sup>3</sup>J(HH) = 12.0, <sup>4</sup>J(HH) = 1.8, <sup>3</sup>J(PH) = 17.1]. <sup>13</sup>C-NMR (CDCl<sub>3</sub>):  $\delta$  30.28 ppm (2C, s, CH<sub>2</sub>SSb), 42.46 ppm (2C, s, CH<sub>2</sub>S), 128.27 ppm [2C, d, C<sub>m</sub>, <sup>3</sup>J(PC) = 14.0], 130.9 (1C, s, C<sub>p</sub>), 131.10 [2C, d, C<sub>o</sub>, <sup>2</sup>J(PC) = 9.3], 137.85 ppm [1C, d, C<sub>i</sub>, <sup>1</sup>J(PC) = 85.8]. <sup>31</sup>P-NMR (CDCl<sub>3</sub>):  $\delta$  56.7 ppm. EI-MS (70 eV): m/z = 370 (Ph<sub>2</sub>PS<sub>2</sub>Sb<sup>+</sup>, 32%), 273 [S(CH<sub>2</sub>CH<sub>2</sub>S)<sub>2</sub>Sb<sup>+</sup>, 8%], 249 (Ph<sub>2</sub>PS<sub>2</sub><sup>+</sup>, 11%), 217 (Ph<sub>2</sub>PS<sup>+</sup>, 100%), 213 [SCH<sub>2</sub>CH<sub>2</sub>SSb<sup>+</sup>, 19%], 185 (Ph<sub>2</sub>P<sup>+</sup>, 26%), 153 (SbS<sup>+</sup>, 12%).

## Crystallographic Section

Single crystals suitable for X-ray diffraction of the oxa and thia-stibocanes **1** and **2** were obtained by diffusion using a CH<sub>2</sub>Cl<sub>2</sub>/n-hexane mixture. The crystallographic and structure solution data for the stibocanes **1** and **2** are summarized in Table 1. A Siemens P4 diffractometer was used, the data were collected in the variable  $\omega$  scan speed with graphite-monochromated MoK $\alpha$  radiation ( $\lambda$  = 0.71073). In both cases corrections were applied for background and Lorentz-polarisation effects, and face indexed absorption correction [22] also. The structures were solved by direct methods, with full-matrix least squares refinement [23] with all non-hydrogen atoms anisotropic and hydrogens in idealized positions with a fixed U<sub>iso</sub> = 0.06 Å<sup>2</sup>. Refined atomic coordinates for the non-hydrogen atoms are collected in Tables 2 and 3.

We thank UNAM-DGAPA for the Grant No. IN100395 and MAMH acknowledges a fellowship from CONACYT.

## References

- [1] M. Dräger, H. J. Guttmann, J. Organomet. Chem. **212** (1981) 171
- [2] H. M. Hoffmann, M. Dräger, J. Organomet. Chem. **295** (1985) 33
- [3] H. M. Hoffmann, M. Dräger, J. Organomet. Chem. **320** (1987) 273
- [4] J. Martin, Jean-Bernard, Acta Crystallogr. **B35** (1979) 1623
- [5] U. Kolb, M. Beuter, M. Dräger, Inorg. Chem. **33** (1994) 4522
- [6] U. Kolb, M. Beuter, M. Gerner, M. Dräger, Organometallics **13** (1994) 4413
- [7] M. Dräger, Z. anorg. allg. Chem. **411** (1975) 79
- [8] R. Cea-Olivares, M. A. Muñoz-Hernández, S. Hernández-Ortega, C. Silvestru, Inorg. Chim. Acta **236** (1995) 31
- [9] M. A. Muñoz-Hernández, R. Cea-Olivares, G. Espinosa-Pérez, S. Hernández-Ortega, J. Chem. Soc., Dalton Trans. submitted for publication
- [10] M. Dräger, Z. anorg. allg. Chem. **424** (1976) 183
- [11] M. Dräger, Z. anorg. allg. Chem. **405** (1974) 183
- [12] M. A. Muñoz-Hernández, R. Cea-Olivares, S. Hernández-Ortega, Inorg. Chim. Acta in press
- [13] W. A. Higgins, P. W. Craig, W. G. Vogel, J. Am. Chem. Soc. **77** (1955) 1894
- [14] I. Haiduc, I. Silaghi-Dumitrescu, R. Grecu, R. Constantinescu, L. Silaghi-Dumitrescu, J. Mol. Struct. **114** (1984) 467
- [15] R. Engler, Z. anorg. allg. Chem. **411** (1975) 79
- [16] R. Engler, Z. anorg. allg. Chem. **406** (1974) 74

- [17] *M. Dräger*, Z. anorg. allg. Chem. **482** (1981) 7
- [18] *I. Haiduc*, Revs. Inorg. Chem. **3** (1981) 353
- [19] *J. D. Smith*, in: Comprehensive Inorganic Chemistry, *A. F. Trotman*, (exec. ed.). Pergamon Press, Oxford, Vol. 2, 1973, p. 591
- [20] *N. N. Greenwood*, *A. Earnshaw*, Chemistry of the Elements, Pergamon Press, Oxford, 1984, p. 652
- [21] *M. Dräger*, Chem. Ber. **114** (1981) 2051
- [22] XSCANS, version 2.0, Siemens Analytical Instruments, Madison, WI (1993)
- [23] SHELXTL PCTM, version 4.1, Siemens Analytical Instruments, Madison, WI, (1990)

## Authors' address:

Dr. Miguel-Angel Muñoz-Hernández,  
Dr. Raymundo Cea-Olivares and Simón Hernández-Ortega  
Instituto de Química  
Universidad Nacional Autónoma de México  
Círculo Exterior, Ciudad Universitaria  
México, 04510, D.F./México  
FAX: 6162217  
e-mail: munozher @ servidodr.unam.mx